Robotics and Computer-Integrated Manufacturing 28 (2012) 366–374

Contents lists available at SciVerse ScienceDirect

Robotics and Computer-Integrated Manufacturing

journal homepage: www.elsevier.com/locate/rcim

Topological localization with kidnap recovery using sonar grid map matching in a home environment

Jinwoo Choi, Minyong Choi, Wan Kyun Chung*

Department of Mechanical Engineering, Pohang University of Science and Technology, San 31, Pohang 790-784, Republic of Korea

ARTICLE INFO

Article history:
Received 14 April 2011
Received in revised form
30 August 2011
Accepted 24 October 2011
Available online 15 November 2011

Keywords:
Topological localization
Kidnap detection
Kidnap recovery
Sonar sensor
Grid-map matching

ABSTRACT

This paper presents a method of topological localization with kidnap recovery capability in a home environment using only low-cost sonar sensors. The proposed method considers both pose tracking and relocation problems. The pose tracking is achieved by calculating node probability using grid-map matching and relative motion model. The relocation method detects the kidnap automatically and recovers it using multiple hypothesis tracking. After kidnap recovery, it also provides a criterion for selecting a reasonable hypothesis for returning to the pose tracking stage autonomously. Experimental results in a real home environment verify that the proposed localization method provides a reliable and convergent node probability when the robot is kidnapped.

1. Introduction

Self-localization is one of the most important capabilities to give an autonomous mobile robot. The mobile robot should recognize its own location in an environmental model to perform autonomous navigation in the environment. The location of the robot can be detected by comparing current sensor data with a known environmental map. For this purpose, many researchers have developed various localization methods, such as Monte Carlo Localization (MCL) [1] and the Extended Kalman Filter (EKF) [2].

The localization of the mobile robot can be classified by pose tracking and relocation. Pose tracking is a localization method for detecting the location of the mobile robot based on a given initial robot pose. Starting from this point, the robot pose is recognized by continuously tracking the robot's path. The current sensor and odometry data can be used for pose tracking. Most localization methods including simultaneous localization and map building (SLAM) algorithms handle the pose tracking problem with various approaches, including feature-based [2,3], and scan-matching-based methods [4].

Relocation entails finding the location of the mobile robot without any initial pose information. When the robot is located at an arbitrary location or kidnapped to an unknown location during pose tracking, the pose of the robot should be detected using only current sensor data. Basically, the relocation problem can be solved by finding the best match of the current sensor data to the known map data. For this purpose, geometric constrains were used for successful matching [5,6], and tracking multiple hypothesis was implemented to handle the relocation problem reliably [7,8]. Some researchers have solved the relocation problem by tracking visual landmarks [9–12].

Pose tracking and relocation should be handled simultaneously to implement the autonomous mobile robot system reliably. The robot should perform successful pose tracking in general situations. When the robot is kidnapped, it should recognize this fact and recover its pose using the relocation algorithm. For this purpose, this paper proposes a localization algorithm that can solve pose tracking and kidnap recovery simultaneously.

The proposed localization method is developed as a topological approach using only low-cost sonar sensors in a home environment. Laser range finders or vision sensors are relatively easier to use than sonar sensors because of their abundant and salient sensor information. Unfortunately, sonar sensors suffer from the noisy data despite of their cost-effectiveness. The noisy data are induced by specular reflections and wide sonar beam-width. These defects make it difficult to directly use raw sonar data for localization. Moreover, feature-based approaches are not easy to apply to localization algorithms using only sonar sensors due to the lower sensor performance. Even though some approaches have been proposed to use sonar sensor for localization and for SLAM with mobile robots [3,13], these approaches

* Corresponding author. Tel.: +82 54 279 2172; fax: +82 54 279 5895.
E-mail addresses: shalomi@postech.ac.kr (J. Choi), minyong@postech.ac.kr (M. Choi), wkchung@postech.ac.kr (W.K. Chung).

0736-5845/$ - see front matter © 2011 Elsevier Ltd. All rights reserved.
doi:10.1016/j.rcim.2011.10.008

also have a potential possibility of failure. For these reasons, this paper proposes a topological localization method based on grid-map matching, assuming a given environmental model.

The construction of the environmental model is adopted from our previous work [14]. The environmental model is acquired using three procedures: (1) generating a grid map for the entire environment using calibrated odometry and sonar data [15], (2) obtaining a draft model of the graphical representation for the empty grids in the grid map using cell decomposition, and (3) extracting subregions by applying normalized graph cut to the draft model. Through these procedures, the environmental model is given by a grid map for the entire environment and a corresponding topological model, as shown in Fig. 1. The topological model represents the extracted subregions in the grid map.

The localization method is developed using sonar grid-map matching based on the given environmental model. The proposed topological localization is composed of a pose tracking stage [16] and a relocation stage. The pose tracking stage performs localization by calculating node probabilities using rotation invariant grid-map matching and a relative motion model, where the former provides reliable observation for the pose tracking, and the latter is used to calculate prior node probability. By applying both of these techniques, the proposed pose tracking provides a convergent node probability.

The relocation stage is conducted by kidnap detection and recovery, where kidnap detection is achieved based on the entropy of the node probability (i.e., when it increases). When the kidnap is detected, it is recovered by generating a new hypothesis. The kidnap recovery process continues to update the original and new hypotheses. While tracking two hypotheses simultaneously, a recovery condition is checked to select a reasonable hypothesis. If the condition is satisfied, one hypothesis is selected for returning to the pose tracking stage, and the other is abandoned.

The proposed method provides convergent and reliable topological localization in a home environment using only low-cost sonar sensors, and it has several advantages. First, the proposed grid-map matching provides a reliable observation by filtering out noisy sonar data in the local grid map. Second, odometry error does not accumulate when the relative motion model is used to calculate the node probability. Third, the proposed kidnap detection procedure can simply detect the kidnapping without any additional sensor information. Finally, the kidnap recovery procedure can solve the relocation problem efficiently and also provides a criterion for returning to the tracking stage automatically.

The remainder of this paper is organized as follows. Section 2 presents the pose tracking process. Section 3 describes kidnap detection and recovery (relocation stage). Section 4 presents experimental results for a real home environment, and Section 5 provides the conclusions.

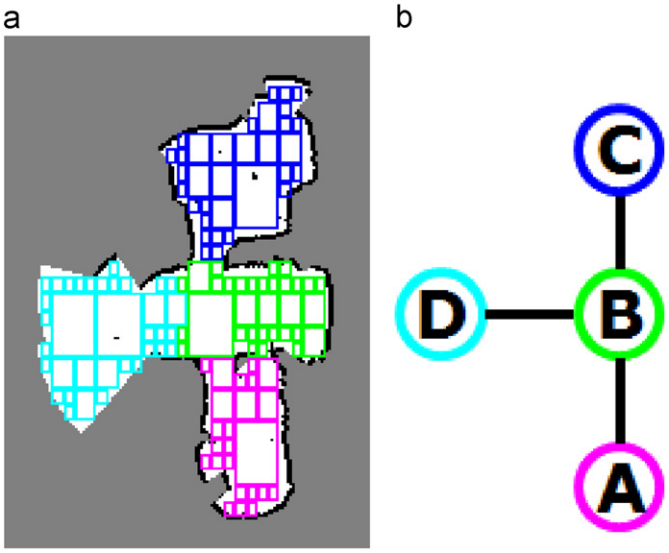

Fig. 1. Example of a topological model: (a) grid map and clustering result (each subregion is represented as a different color) and (b) corresponding topological model. (For interpretation of the references to color in this figure legend, the reader is referred to the web version of this article.)

2. Pose tracking of topological localization

This section describes the pose tracking stage of the proposed topological localization method. The pose tracking method is adopted from our previous work [16] with some modifications. The proposed method is performed based on grid-map matching. A local grid map generated around the current robot position is compared with the grid map given by the environmental model. Then, the pose tracking takes place in three steps: (1) extracting a template grid map to filter out noisy data; (2) obtaining candidate locations and matching probabilities using rotation invariant grid-map matching; and (3) calculating node probabilities using the matching probabilities and the relative motion model. The pose tracking method provides convergent localization by calculating node probabilities using a Bayesian update process.

2.1. Extracting the template grid map

The local grid map generated around the current robot location will contain noisy data, as shown in Fig. 2(a), when there are insufficient sensor data to filter out the noisy data. Therefore, the template grid map is first extracted to filter out the noisy data. The extraction of the template grid map is performed by measuring the grid confidence of each grid in the local grid map.

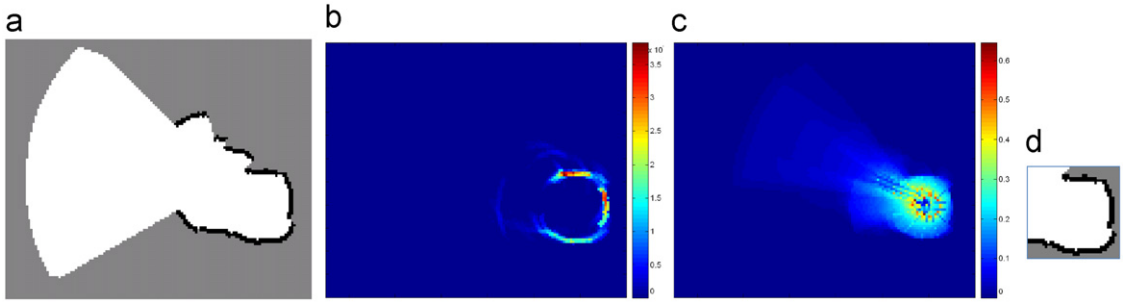

Fig. 2. Extraction of the template grid map: (a) noisy local grid map, (b) grid confidence for occupied grids, (c) grid confidence for empty grids, and (d) extracted template grid map.

The confidence for a grid (x,y) is defined as follows:

$$Conf(x,y) = \sum_{s \in S_{xy}} P_s(r,\theta), \tag{1}$$

where s is each sensor measurement, S_{xy} is a set of sensor measurements whose sensing range includes the grid (x,y), and P_s is a sound pressure function of a sonar sensor (2), given by:

$$P_s(r,\theta) = \frac{\beta f a^4}{r^2}\left(\frac{2J_1(ka\sin\theta)}{ka\sin\theta}\right)^2, \tag{2}$$

where r and θ are the distance and angle of the grid (x,y) with respect to the transmitter. Detailed explanations for the other variables can be found in [17].

The grid confidence is acquired for all occupied and empty grids separately. Then, the grids with above-average grid confidences are classified as confident grids, and the other grids are regarded as noisy data. Fig. 2(b) and (c) shows grid confidences for the occupied and empty grids, respectively. By extracting a region that includes confident grids, a template grid map is obtained. Fig. 2(d) is a template grid map extracted from the local grid map of Fig. 2(a).

2.2. Rotation invariant grid map matching

The extracted template grid map is matched to the original grid map of the given environmental model. Through grid map matching, candidate locations are selected from each node, and corresponding matching probabilities are acquired.

Grid-map matching is performed by Ring Projection Transformation (RPT) [18], which transforms 2D image data into a 1D vector, as shown in Fig. 3. The RPT vector for the template grid map is obtained with respect to the center point of the template grid map, and RPT vectors for the original grid map are acquired with respect to every grid within each node. Then, grid-map matching is achieved by calculating the normalized correlation between the RPT vector of the template grid map ($P_T(r)$) and the RPT vectors of the original grid map ($P_O(r)$) (3), as follows:

$$\rho = \frac{\sum_{r=0}^{R}\{P_T(r)-\mu_T\}\{P_O(r)-\mu_O\}}{(\sum_{r=0}^{R}\{P_T(r)-\mu_T\}^2 \cdot \sum_{r=0}^{R}\{P_O(r)-\mu_O\}^2)^{1/2}}, \tag{3}$$

where R is the size of the RPT vector, $\mu_T = \sum_{r=0}^{R} P_T(r)/(1+R)$, and $\mu_O = \sum_{r=0}^{R} P_O(r)/(1+R)$. The size of the RPT vector is set to be half the width of the template grid map.

Using grid-map matching, candidate locations are obtained as the maximum normalized correlation point within each node. The candidate locations become representative points of each node for the localization.

Then, a distance vector $D(\theta)$ and an angle vector $A(\theta)$ are used to acquire more salient matching probabilities, where the former represents the distance to the closest obstacle for each direction, and each element of the latter has a value of 0 or 1 and represents the existence of obstacles in each direction. Using these vectors for the template grid map and candidate locations, the similarity of the distance and angle vectors for the ith candidate location (x_i,y_i) is obtained as follows:

$$P_{DA}(i) = \frac{1/\Delta DA_i}{\sum_j 1/\Delta DA_j}, \tag{4}$$

where

$$\Delta DA_i = \arg\min_{\theta_c} \sum_{\theta=1}^{360} |D_T(\theta)-D_i(\theta-\theta_c)| \times |A_T(\theta)-A_i(\theta-\theta_c)|. \tag{5}$$

Finally, the matching probability for the ith node can be calculated by multiplying the normalized correlation of the RPT vectors and the similarity, as follows:

$$P_{match}(i) = \rho(x_i,y_i) \times P_{DA}(i). \tag{6}$$

2.3. Calculating node probability

Pose tracking is achieved by calculating node probabilities using Bayesian update for observations and robot motion models (7), as follows:

$$P(N_t = N_i | u_{1:t}, z_{1:t}) = \eta_1 P(z_t | N_t = N_i) P(N_t = N_i | u_{1:t}, z_{1:t-1}), \tag{7}$$

where η_1 is a normalizing factor, N_t is the node where the robot is located at time t, N_i is the ith node, and $u_{1:t}$ and $z_{1:t}$ are the robot's motions and the observations up to time t, respectively. The first part of (7) is a likelihood, which can be replaced with the matching probability of (6). The last part of (7) is a prior node probability, which can be obtained from the robot motion model and the previous node probability as follows:

$$\begin{aligned} P(N_t = N_i | u_{1:t}, z_{1:t-1}) &= \sum_j P(N_t = N_i | N_{t-1} = N_j, u_{1:t}, z_{1:t-1}) \\ &\quad \times P(N_{t-1} = N_j | u_{1:t-1}, z_{1:t-1}). \end{aligned} \tag{8}$$

In the motion model, relative distance and relative angle are used. Even though the robot moves along an arbitrary path such as that shown in Fig. 4(a), only relative distance and angle are used, as shown in Fig. 4(b). We call these Effective Distance (ED) and Effective Angle (EA), which are acquired from the locations at which the current local grid map is generated. Using ED and EA, the first part of (8) can be derived as follows:

$$\begin{aligned} &P(N_t = N_i | N_{t-1} = N_j, ED_{1:t}, EA_{1:t}, z_{1:t-1}) \\ &\quad = \eta_2 P(N_t = N_i | N_{t-1} = N_j, ED_{1:t}, EA_{1:t-1}, z_{1:t-1}) \\ &\qquad \times P(N_t = N_i | N_{t-1} = N_j, ED_{1:t-1}, EA_{1:t}, z_{1:t-1}) \\ &\quad = \eta_2 P(N_t = N_i | N_{t-1} = N_j, ED_t) \\ &\qquad \times \sum_k P(N_t = N_i | N_{t-1} = N_j, N_{t-2} = N_k, EA_t) \\ &\qquad \times P(N_{t-2} = N_k | N_{t-1} = N_j, u_{1:t-1}, z_{1:t-1}), \end{aligned} \tag{9}$$

where η_2 is a normalizing factor. More details of the derivation using relative motion models can be found in [16].

Through Bayesian update using the relative motion model, the proposed pose tracking can provide a convergent node probability. The proposed topological localization method does not directly estimate metric information (x,y,θ) of the robot with

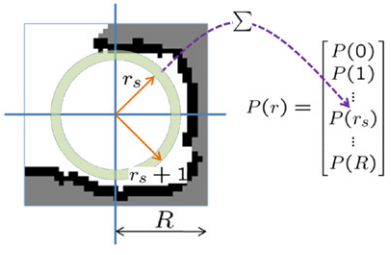

Fig. 3. Ring projection transformation using the extracted template grid map.

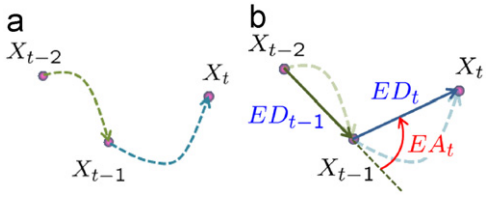

Fig. 4. Robot motion model: (a) actual robot motion and (b) effective distance (ED) and effective angle (EA).

respect to a reference coordinate. Instead, to achieve the relative motion model, candidate locations of two previous time steps are maintained in grid resolution with respect to a given grid map. The accumulation of odometry error is bounded in two time steps using this relative motion model.

As mentioned, the pose tracking method is based on our previous work [16] with two modifications. First, the proposed method extracts template grid maps using grid confidences of both occupied and empty grids, while the previous method used only occupied grids. Using the grid confidences of both occupied and empty grids, the template grid map is extracted as a square that includes confident grids within the inscribed circular area of the square. Second, an angle vector is defined and used to obtain the matching probability. Because it uses both distance and angle vectors simultaneously, the proposed method can provide more salient matching probability.

3. Relocation of topological localization

The proposed pose tracking process provides reliable results for topological localization. However, the autonomous mobile robot might occasionally be kidnapped during operation. When the robot is suddenly moved to an unknown location, the pose tracking method will fail to find the correct location because the previous node probability provides wrong information. To cope with this problem, we expand the topological localization algorithm by adding a relocation stage composed of kidnap detection and kidnap recovery.

3.1. Kidnap detection

When the robot is kidnapped, the robot should recognize this fact so that it can perform the recovery process effectively. In the proposed relocation stage, the entropy of the node probability is measured to detect the kidnap (10), as follow:

$$H(P) = \sum_{i=1}^{n} -P(i)\log_n P(i), \tag{10}$$

where n is the number of nodes in the topological model, and $P(i)$ is the node probability of the ith node.

The entropy of the node probability reflects the convergence of the node probability. For the uniformly distributed node probability ($P(i) = 1/n$ for all i), the entropy becomes 1. On the other hand, the entropy becomes 0 for the perfectly converged node probability ($P(i) = 1$ and $P(j) = 0$ for all $j \neq i$). In other words, more convergence results in less entropy. In a general pose tracking procedure, a successful observation should induce a convergent node probability. That is, the entropy should decrease as the node probability is updated.

When the robot is kidnapped, grid-map matching cannot provide a reliable observation to acquire the convergent node probability. This unreliable matching probability might increase the entropy of the node probability. If the robot is kidnapped from the ith node to the jth node between time step $t-1$ and t, the generated local grid map at time step t contains sonar data obtained from both the ith node and the jth node. Therefore, the local grid map at time step t gives an unreliable observation. This results in divergence of the node probability, and the entropy increases at time step t, as shown in Fig. 5. Using this relationship between the node probability and its entropy, the kidnap can be detected by checking whether the entropy increased or not. If the entropy increases at time step t, we can assume that the robot may have been kidnapped between time step $t-1$ and t.

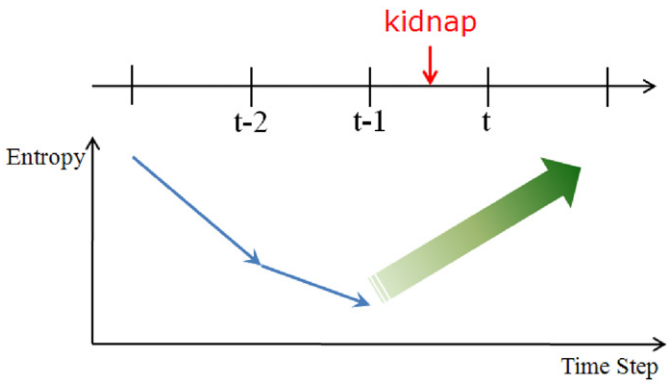

Fig. 5. Entropy of node probability when the robot is kidnapped.

3.2. Kidnap recovery

Variation in the entropy measure indicates the possibility of kidnap. When kidnapping is detected, the robot should verify it and attempt to recover it. Then, the localization algorithm should return to the pose tracking stage. To achieve these objectives, the proposed kidnap recovery process uses the concept of multiple hypothesis tracking to acquire a reliable node probability and to provide a criterion for returning to the pose tracking stage.

When the entropy of the node probability increases, there are two possible causes: (1) the robot is actually kidnapped or (2) the node probability is temporarily disturbed by a failure in grid-map matching. If the robot is truly kidnapped, it should calculate the node probability using sensor data acquired after the kidnap because the information before the kidnap is useless. On the other hand, if the robot is not kidnapped, but rather, the node probability is temporarily disturbed by unsuccessful grid map matching, then the robot can correct the node probability using subsequent sensor information. The proposed kidnap recovery process considers both cases simultaneously to provide reliable topological localization.

3.2.1. Actual kidnap case

When a kidnap is detected, a new hypothesis with a uniformly distributed node probability is generated, as follows:

$$P_{new}(i) = \frac{1}{n} \quad \text{for all } i, \tag{11}$$

where n is the number of nodes in the topological model.

If a kidnap is detected at time step t, the uniform node probability set is generated at that time step. Then, the newly generated node probability set is updated using the sensor data after the time step at which the kidnap was detected. In other words, the new node probability set is first updated at time step $t+1$ using the local grid map generated from the sensor data between time step t and $t+1$. The node probability update is achieved by the general pose tracking method described in Section 2.

3.2.2. False kidnap case

While tracking the new hypothesis, the original node probability set is simultaneously updated to consider the possibility of temporary failure in grid-map matching, which could be due to an insufficient local grid map. In this case, the robot can recover the temporary failure by accumulating more sensor data to obtain a more reliable local grid map. To this end, the original hypothesis does not update the node probability at time step t when the entropy increases. Instead, the robot accumulates more sensor data until time step $t+1$ and expands the local grid map.

Then, this expanded local grid map is used to update the original node probability set at time step $t+1$.

After that time step, both the original and new node probability sets are simultaneously updated using the same sensor data. By tracking both hypotheses, we can consider two possible cases for kidnap detection.

3.2.3. Selecting a reasonable hypothesis

During multiple hypothesis tracking, the robot should select one hypothesis for returning to the pose tracking stage. To select the most reasonable hypothesis, the kidnap recovery process evaluates two hypotheses and proposes a selection criterion. The evaluation of the two hypotheses is accomplished using two measures: the entropy of each node probability set and the probability of a specific node that best matches the sensor data acquired after kidnap detection. These measures are used to select one hypothesis and to determine whether to return to the pose tracking stage.

As previously mentioned, the entropy reflects the convergence of the node probability set. Had the robot truly been kidnapped, the new hypothesis would give a more convergent node probability than the original one. The original node probability set might result in slow convergence because the node probability before the kidnap does not represent accurate information. As a result, the entropy of the new node probability set ($H(P_{new})$) will be smaller than that of the original node probability set ($H(P_{ori})$). On the other hand, in the case of a false kidnap, the entropy of the new hypothesis will be larger than that of the original one. Even though the entropy of the original node probability set is temporarily disturbed by the matching failure, the original hypothesis can recover its convergence by acquiring a more reliable local grid map by accumulating more sensor data. Therefore, the hypothesis that produces the smallest entropy can be considered the most reasonable.

As the second measure, the probability of a specific node is compared. The node is determined as the best-matched node to the sensor information acquired after kidnap detection. To do this, a matching probability ($P_{b.m}$) is calculated for each node using the motion models and observations, and the best matched node ($i_{b.m}$) is considered the one with the highest probability value (12). The observations and the motion models in (12) are obtained from the sensor data after kidnap detection:

$$P_{b.m}(i) = \arg\max_{j,k}\{P(z_t|N_t=N_i)\times P(z_{t-1}|N_{t-1}=N_j) \times P(z_{t-2}|N_{t-2}=N_k)\times P(N_t=i|N_{t-1}=j,ED_t) \times P(N_{t-1}=j|N_{t-2}=k,ED_{t-1})\times P(N_t=i|N_{t-1}=j,N_{t-2}=k,EA_t)\}. \quad (12)$$

The first row of (12) is the matching probability of the observation models (grid-map matching) and the second and last rows represent the matching probability of the motion models. Using the best matched node $i_{b.m}$, the hypothesis with greatest probability of the node $i_{b.m}$ is considered the most reasonable hypothesis.

Using the entropy and the node probability of $i_{b.m}$, the kidnap recovery process selects the most reasonable hypothesis for returning to the pose tracking stage. The selection criterion is shown in Fig. 6. In the bottom-right panel, the kidnap recovery process concludes that the robot is truly kidnapped, and it selects a new hypothesis if that hypothesis shows less entropy and a greater node probability of $i_{b.m}$ than the original hypothesis. In the top-left panel, the robot concludes that the kidnap detection is false and selects the original node probability for returning to the pose tracking stage. The robot considers the other cases undeterminable, and thus the kidnap recovery process is performed continuously until the condition is satisfied. The proposed method provides an effective criterion for selecting a reasonable hypothesis for returning to the pose tracking stage automatically.

	$H(P_{new}) > H(P_{ori})$	$H(P_{new}) < H(P_{ori})$
$P_{ori}(i_{b.m}) > P_{new}(i_{b.m})$	False kidnap	Undeterminable
$P_{ori}(i_{b.m}) < P_{new}(i_{b.m})$	Undeterminable	Actual Kidnap

Fig. 6. A criterion for selecting a hypothesis for returning to the pose tracking stage.

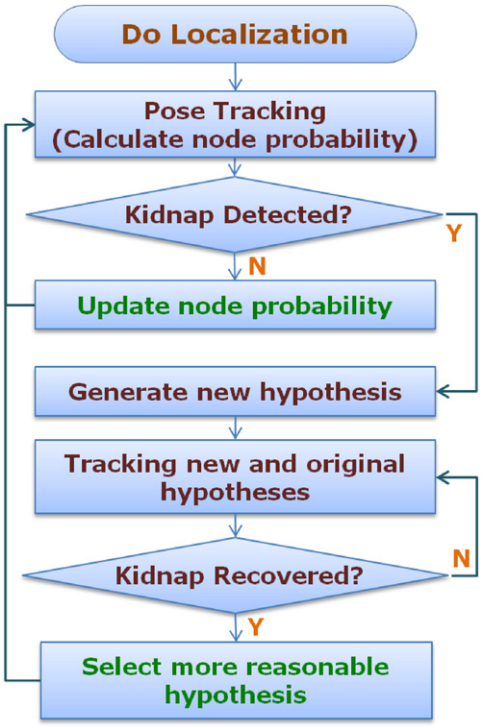

Fig. 7. Flowchart of the proposed relocation algorithm.

Fig. 7 shows a brief flowchart of the proposed topological localization with kidnap recovery. Through the pose tracking and relocation methods, the robot can perform successful topological localization even when the robot is kidnapped.

4. Experimental results

This section provides the experimental results of the proposed pose tracking and kidnap recovery algorithms. Experiments were conducted in a real home environment as shown in Fig. 8(a). The home environment is 11.4 m × 8.7 m area and consists of three rooms, a kitchen, and a living area. We used a differential drive robot, PIONEER3-DX, equipped with 12 MA40B8 sonar sensors from the MURATA company, as shown in Fig. 8(b). The environmental model for the experiments is shown in Fig. 9; it includes a grid map of the entire environment and a topological model represented by 10 subregions. In the experiment, the mobile robot was driven along an arbitrary path manually at an average speed of about 0.15 m/s, and sensor data were acquired at a frequency of 4 Hz.

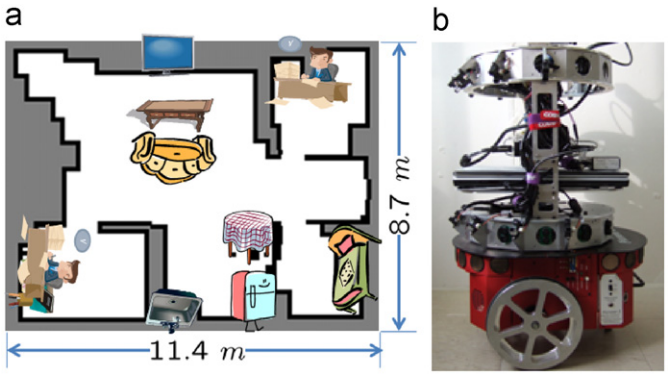

Fig. 8. Experimental setup: (a) home environment in which the experiments were conducted and (b) pioneer 3-DX equipped with 12 Murata sonar sensors.

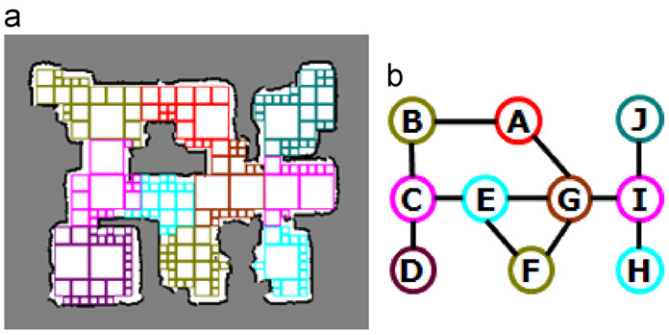

Fig. 9. Experimental model: (a) grid map with extracted subregions and (b) topological model.

4.1. Grid-map matching results

Fig. 10 shows the performance of the proposed grid map matching method prior to the pose tracking and relocation experiment. The robot moved about 1.5 m along its path and acquired a local grid map around its position. As shown in Fig. 10(a) and (b), the template grid maps were extracted properly by filtering out noisy data in the local grid map, and the proposed grid map matching method resulted in successful matching even under rotational changes.

Fig. 10(c) and (d) shows node probabilities obtained using only RPT vector matching (3). Even though RPT vector matching can be used to select reliable candidate locations from the subregions, it is not sufficient to provide a salient matching probability. Fig. 10(e) and (f) shows the node probabilities calculated using both RPT vector matching and distance and angle vector matching (6). Distance and angle vector matching thus provides more salient matching probability, which can be used to perform successful pose tracking and relocation.

4.2. Localization results

Fig. 11 shows the path the robot took during the localization experiment. The robot experienced two kidnaps during the experiment: $P1 \rightarrow P1'$, during which the robot was moved from node H to node D, and $P2 \rightarrow P2'$, during which the robot was moved from node B to node F. As it moved, it generated local grid maps and calculated node probability to perform localization using the proposed pose tracking and relocation methods. The size of the local grid map was determined by both traveling time and distance. The traveling distance for each local grid map was approximately 1.5–2.0 m.

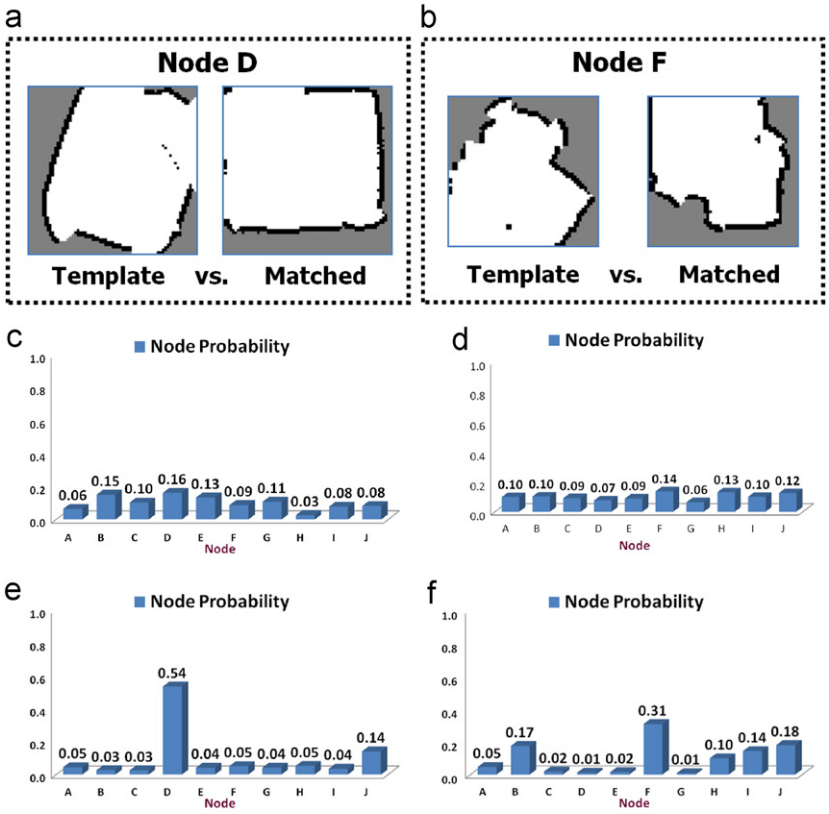

Fig. 10. Experimental results of grid map matching: (a) and (b) extracted template grid map and grid map matching results, (c) and (d) matching probability using only RPT vector matching, and (e) and (f) matching probability using both RPT vector and distance and angle vectors.

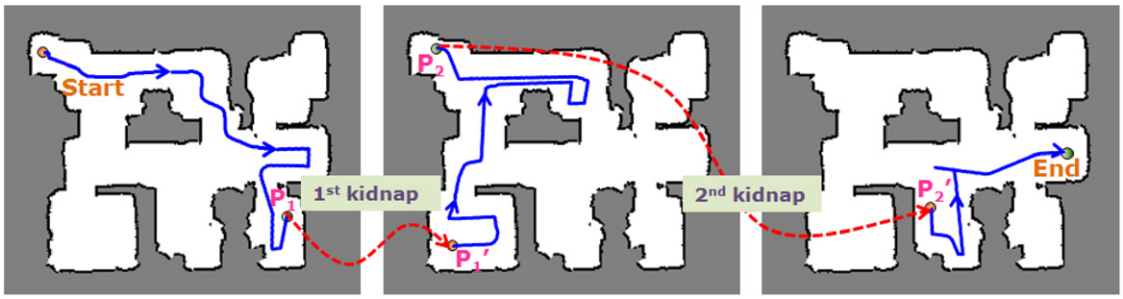

Fig. 11. Path of the robot during the localization experiment.

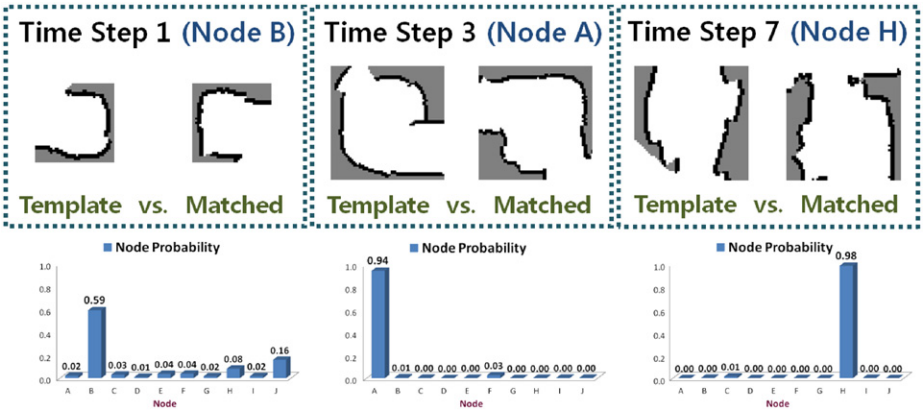

Fig. 12. Experimental results of pose tracking before the first kidnap.

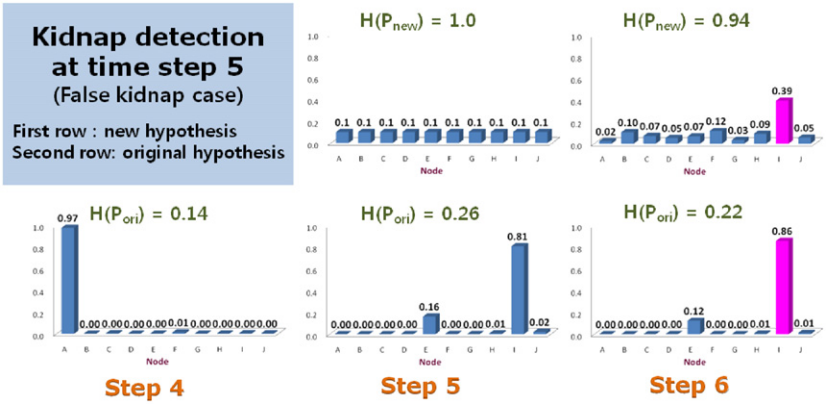

Fig. 13. Kidnap recovery process for the false-kidnap case. The magenta node probabilities at time step 6 represent the probabilities of the best matched node. (For interpretation of the references to color in this figure legend, the reader is referred to the web version of this article.)

The experimental results of the proposed pose tracking, including grid-map matching and corresponding node probabilities before the first kidnap, are shown in Fig. 12. As shown, the robot achieved successful localization using reliable grid-map matchings. Moreover, the node probability verified that the proposed pose tracking method provided convergent localization as the Bayesian update was performed.

Figs. 13 and 14 show the kidnap recovery processes for false-kidnap and actual kidnap, respectively. The upper row of each figure shows the node probability of the newly generated hypothesis, and the lower row shows the node probability of the original hypothesis.

As shown in Fig. 13, a new hypothesis was generated at time step 5 because the entropy increased. Through the kidnap recovery process of the relocation stage, two hypotheses were updated at time step 6. The obtained node probabilities at time step 6 were tested by the recovery criterion shown in Fig. 6. The case was determined to be a false-kidnap because the original hypothesis had less entropy and a higher probability of the best-matched node (magenta bars) than the new hypothesis did. As a result, the new hypothesis was abandoned at time step 6, and the localization algorithm returned to the pose tracking stage with the original hypothesis at time step 7.

Another kidnap was detected at time step 9, as shown in Fig. 14. In fact, the kidnap detection was induced by the first kidnap (node H→D). As the robot was kidnapped, the entropy of the original node probability increased dramatically at time step 9. The relocation process began at that time, and two hypotheses were updated simultaneously. After tracking two time steps, the selection criterion was satisfied at time step 11. As shown, the new hypothesis had a higher probability of the best-matched node with smaller entropy than the original hypothesis.

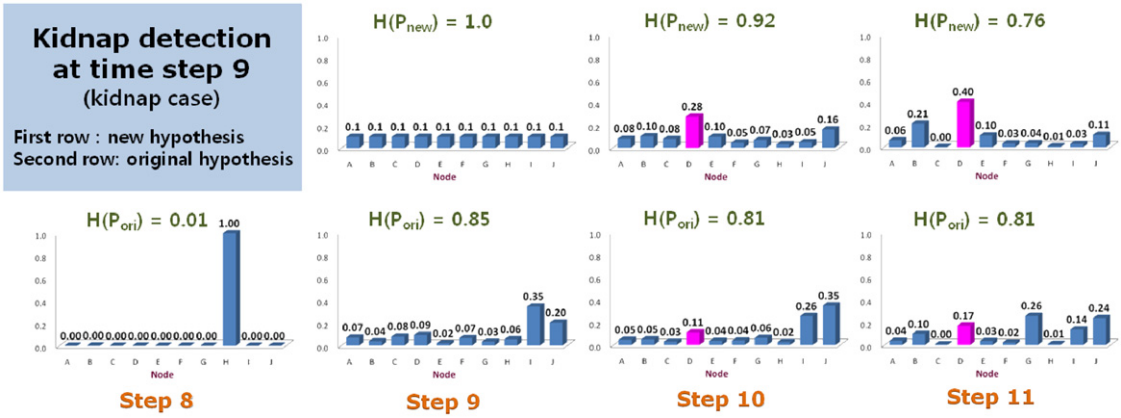

Fig. 14. Kidnap recovery process for the actual kidnap case. Kidnap was detected at time step 9, and the kidnap was recovered at time step 11 by satisfying the criterion shown in Fig. 6. The magenta node probabilities at time steps 10 and 11 represent the probabilities of the best matched node. (For interpretation of the references to color in this figure legend, the reader is referred to the web version of this article.)

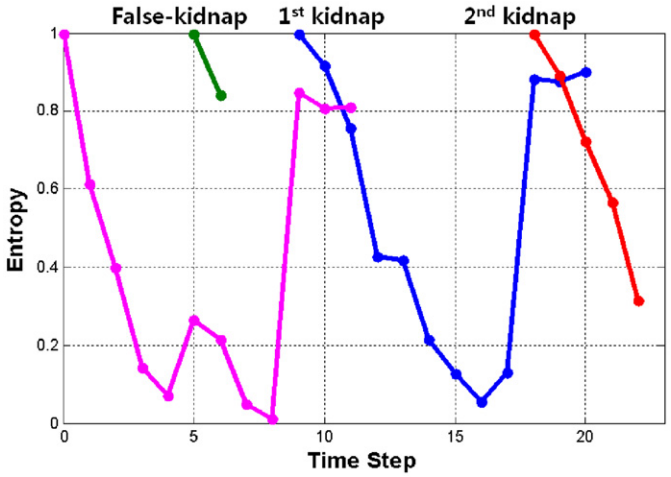

Fig. 15. Entropy of node probability. Three potential kidnaps were detected, and therefore new hypotheses were generated at time steps 5, 9, and 18.

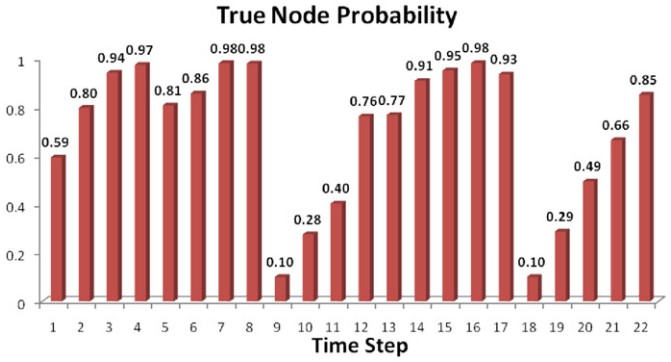

Fig. 16. True node probability.

Therefore, the new hypothesis was selected as the more reasonable one, and the localization algorithm returned to the pose tracking stage with the new hypothesis. This result verifies that the proposed relocation method can reliably detect kidnaps using the entropy measure and can recover the kidnap using multiple hypothesis tracking and the proposed selection criterion.

Fig. 15 shows the entropy of the node probabilities for all time steps. Potential kidnaps were detected three times, at time steps 5, 9, and 18. That at time step 5 was considered a false kidnap, and that at time step 9 was concluded to have been induced by the first kidnap. The kidnap at time step 18 was correctly identified as a true kidnap, and recovery was successfully achieved. Fig. 16 shows the true node probability. The proposed relocation method rapidly recovered a convergent node probability as the robot performed the kidnap recovery process.

A kidnap was not detected even though the entropy increased at time step 17. The kidnap detection process is performed only when the maximum node probability is smaller than some threshold value, which in this case was 0.9. If the maximum node probability is greater than the threshold value, we assume that the node probability is sufficiently converged and that the robot has not been kidnapped. As shown in Fig. 16, the kidnap detection process did not take place because the maximum node probability was 0.93.

4.3. Long-term experiment of the topological localization

An additional experiment was conducted to verify the performance of the proposed topological localization method for long-term operation. In this experiment, the robot moved along an arbitrary path and experienced 10 times the number of kidnaps.

Table 1 shows the experimental results of the long-term experiment including the time steps at which kidnaps were detected, the required number of time steps to recover from the detected kidnaps, and the decision to select the more reasonable hypothesis. Twelve kidnaps were detected as shown, two of which were considered to be false kidnap. In those cases, the robot returned to the pose tracking stage with the original node probability set. The 10 kidnap detections were determined to be actual kidnap based on the criterion in Fig. 6. In these cases, the original node probability sets were abandoned and the robot returned to the pose tracking stage using the new node probability set.

These 10 occurrences of actual kidnap were detected immediately, except for that at time step 27. In that case, the robot was actually kidnapped between time steps 25 and 26. However, the local grid map at time step 26 contained much sensor data that had accumulated before the kidnap took place. For this reason, the kidnap detection was slightly delayed until time step 27. Even though the kidnap was not detected immediately, it was detected at the subsequent time step and recovered reliably. As shown in Table 1, all of the detected kidnaps were recovered within 2–4 time steps after detection. These experimental results show that the proposed kidnap detection and recovery algorithm works well in various kidnapping situations.

Table 1
Experimental results of kidnap detection and recovery.

Time step when kidnap was detected	Required time steps to recover detected kidnap	Decision
5	2	Actual kidnap
10	2	False kidnap
13	3	Actual kidnap
20	3	Actual kidnap
27	4	Actual kidnap
34	2	Actual kidnap
41	3	Actual kidnap
48	3	Actual kidnap
53	2	Actual kidnap
58	2	False kidnap
61	3	Actual kidnap
70	3	Actual kidnap

The above experimental results verify the performance of the proposed topological localization. The proposed method performed successful localization in a real home environment even when the robot was kidnapped. For the topological localization, both the pose tracking and relocation stages worked complementarily to provide a reliable result.

5. Conclusions

This paper described a method of topological localization with kidnap recovery capability. The proposed method provides a reliable topological localization method in a home environment using only low-cost sonar sensors. By considering pose tracking and relocation at the same time, robots that use the proposed method can manage kidnapping autonomously.

The contributions of this paper are as follows. First, successful pose tracking can be achieved using reliable grid map matching and relative motion models. Second, the relocation stage can detect and recover kidnaps effectively using the concept of multiple hypothesis tracking. Finally, the kidnap recovery process provides a reliable criterion for selecting a reasonable hypothesis for returning to the pose tracking stage.

The experimental results verified that the proposed method can be applied to a real home environment to provide convergent localization even when the robot is kidnapped.

Acknowledgments

This work was supported in part by National Research Foundation of Korea (NRF) grant funded by the Korea government (MEST) (No. 2011-0030075), in part by the "Development of mobile assisted robot and emotional interaction robot for the elderly (10038574)" under the Industrial Source Technology Development Programs of the Ministry of Knowledge Economy (MKE) of Korea, in part by the Global Frontier R&D Program on Human-centered Interaction for Coexistence funded by the National Research Foundation of Korea grant funded by the Korean Government (MEST) (NRF-M1AXA003-2010-0029748), in part by the Acceleration Research Program of the Ministry of Education, Science and Technology of the Republic of Korea and the National Research Foundation of Korea (R17-2008-021-01000-0), and in part by UTRC (Unmanned technology Research Center) at KAIST (Korea Advanced Institute of Science and Technology), originally funded by DAPA, ADD.

References

[1] Thrun S, Fox D, Burgard W, Dellaert F. Robust Monte Carlo localization for mobile robots. Artificial Intelligence 2001;128(1–2):99–141.
[2] Leonard JJ, Durrant-Whyte HF. Mobile robot localization by tracking geometric beacons. IEEE Transactions on Robotics and Automation 1991;7(3):376–82.
[3] Tardós JD, Neira J, Newman PM, Leonard JJ. Robust mapping and localization in indoor environments using sonar data. International Journal of Robotics Research 2002;21(4):311–30.
[4] Gutmann JS, Konolige K. Incremental mapping of large cyclic environments. In: Proceedings of IEEE international symposium on computational intelligence in robotics and automation; 1999. p. 318–25.
[5] Lim JH, Leonard JJ. Mobile robot relocation from echolocation constraints. IEEE Transactions on Pattern Analysis and Machine Intelligence 2000;22(9):1035–41.
[6] Neira J, Tardós JD, Castellanos JA. Linear time vehicle relocation in SLAM. In: Proceedings of IEEE international conference on robotics and automation; 2003. p. 427–33.
[7] Jensfelt P, Kristensen S. Active global localization for a mobile robot using multiple hypothesis tracking. IEEE Transactions on Robotics and Automation 2001;17(5):748–60.
[8] Arras KO, Castellanos JA, Schilt M, Siegwart R. Feature-based multi-hypothesis localization and tracking using geometric constraints. Robotics and Autonomous Systems 2003;44(1):41–53.
[9] Albert ME, Connell JH. Visual rotation detection and estimation for mobile robot navigation. In: Proceedings of IEEE international conference on robotics and automation; 2004. p. 4247–52.
[10] Williams B, Smith P, Reid ID. Automatic relocalisation for a single-camera simultaneous localisation and mapping system. In: Proceedings of IEEE international conference on robotics and automation; 2007. p. 2784–90.
[11] Gasparri A, Panzieri S, Priolo A. A fitness-sharing based genetic algorithm for collaborative multi-robot localization. Intelligent Service Robotics 2010;3(3):137–49.
[12] Pathak K, Vaskevicius N, Birk A. Uncertainty analysis for optimum plane extraction from noisy 3D range-sensor point-clouds. Intelligent Service Robotics 2010;3(1):37–48.
[13] Yap TN, Shelton CR. SLAM in large indoor environments with low-cost, noisy, and sparse sonars. In: Proceedings of IEEE international conference on robotics and automation; 2009. p. 1395–401.
[14] Choi J, Choi M, Chung WK. Incremental topological modeling using sonar gridmap in home environment. In: Proceedings of IEEE/RSJ international conference on intelligent robots and systems; 2009. p. 3582–7.
[15] Lee K, Chung WK. Effective maximum likelihood grid map with conflict evaluation filter using sonar sensors. IEEE Transactions on Robotics 2009;25(4):887–901.
[16] Choi J, Choi M, Nam SY, Chung WK. Autonomous topological modeling of a home environment and topological localization using a sonar grid map. Autonomous Robots 2011;30(4):351–68.
[17] Kleeman L, Kuc R. Sonar sensing. In: Siciliano B, Khatib O, editors. Handbook on robotics. Springer-Verlag; 2008.
[18] Lin Y, Chen C, Wei C. New method for subpixel image matching with rotation invariance by combining the parametric template method and the ring projection transform process. Optical Engineering 2006;45(6):067202. (1–9).